LIFT ON TWO-DIMENSIONAL SYMMETRICAL AIRFOIL OF FINITE THICKNESS IN SUPERSONIC FLOW

Thesis by

Ting-Yi Li

In Partial Fulfillment of the Requirements for the

Degree of Aeronautical Engineer

California Institute of Technology

Pasadena, California

May, 1947

Acknowledgement

The author wishes to express his profound indebtedness to Mr. A. E. Puckett who inspired and directed this research. The author also wishes to thank Drs. H. J. Stewart and C. DePrima for their suggestions and criticisms.

Table of Contents

Summary :

This research consists of a study of several methods of computing the slope of lift curve for a two-dimensional symmetrical airfoil of finite thickness in completely supersonic potential flow. An "exact" formula is derived by considering the flow conditions over the airfoil surface including the effects of the oblique shock waves emitted from the leading edge of the airfoil. This "exact" formula is applied to two simple cases : (1) a 5% thick circular arc airfoil, and (2) a 10% thick circular arc airfoil. The computation results are compared with (1) Ackeret's linearized theory, (2) Busemann's second order theory and (3) Busemann's third order theory. It is found that the presence of shock waves at the airfoil leading edge will lead to a reversal in sign of the slope of lift curve at low Mach numbers close to 1.00, this effect is also sometimes observed experimentally. Furthermore, it has been shown that the linearized theory and the second order theory give too low $dC_L/d\alpha$ values at high Mach numbers. The third order theory agrees with the "exact" theory in general tendency but is not quite so accurate in very high Mach number region and at Mach numbers close to 1.00. Thus, for accurate determination of the slope of lift curve , the "exact" formula may find some engineering uses. To facilitate future computations, charts for the necessary coefficients are prepared and steps in applying the formula for engineering cases are outlined and discussed in some detail.

Symbols :

$(\ )_\infty$ conditions in free stream, i. e. ahead of the oblique shock,

$(\ )_2$ conditions immediately behind the oblique shock,

Free stream conditions :

M_∞ Mach number

p_∞ static pressure

w_∞ velocity

a_∞ sound velocity

q_∞ dynamic pressure

ϱ_∞ density

$p_{o\infty}$ stagnation pressure

Conditions at 2 :

M_2 Mach number

p_2 static pressure

w_2 velocity

θ_2 Prandtl-Meyer angle

p_{o2} stagnation pressure

Local conditions over the airfoil :

M Mach number

p static pressure

w velocity

θ Prandtl-Meyer angle

ϱ density

Angles :

ε expansion angle between two adjacent elements of the airfoil surface

β wave angle of the oblique shock

α angle of attack

ϕ flow deflection due to the oblique shock

2ψ vertex angle of the airfoil

γ ratio of specific heats of air

a^* critical speed of sound

τ airfoil thickness ratio

$\frac{x}{c}$ running airfoil chord ratio

P total pressure on the upper surface of the airfoil

L lift force

C_p pressure cefficient:

C_{pi} in isentropic flow

C_{ps} in oblique shock flow

Introduction :

It is well-known that in a completely supersonic steady flow the partial differential equation governing the flow is of the hyperbolic type. A given disturbance cannot be propagated forward into the field; in fact, there exists the Mach line or the characteristic line on one side of which the disturbance produces no effects. (Ref. 1, 2) Based upon this principle and neglecting the effects of viscous boundary layer, the supersonic flow past a two-dimensional airfoil of finite thickness can be determined by a step by step calculation. The conditions at any point on the airfoil surface depends only on the geometry of the surface. They can be calculated for all points on the surface if the conditions at one point are known. It is usually observed in wind tunnel experiments that an oblique shock wave is emitted at the leading edge of an airfoil in supersonic flow. This oblique shock wave represents an irreversible adiabatic process. If the shock strength is not too strong, as for example the oblique shock wave created at the leading edge of an airfoil at low angle of attack, it has been shown that the flow before and after the shock wave is essentially isentropic. (Ref. 3) In such case, as before, the step by step calculation method can be used to obtain information about the airfoil characteristics as long as the airflow before and after the shock is everywhere supersonic. Knowing the free stream conditions i. e. the conditions far away ahead of the airfoil, the oblique shock formulae will

give a definite solution for the conditions at the surface of the airfoil immediately after the shock at the leading edge. Having calculated the conditions immediately after shock, it is possible to apply the Prandtl-Meyer expansion law to determine the conditions at all points on the airfoil with the understanding that flow is everywhere supersonic and isentropic after the shock, and that the boundary layer effects are neglected. It is the purpose of this present research to carry out a calculation of this nature in order to determine the behavior of the slope of lift curve for a two-dimensional symmetrical airfoil in supersonic flight. However, for calculation of the slope of lift curve for an airfoil, it is more convenient to deal directly with the differential increment of pressure on the airfoil surfaces with respect to the differential increment of the angle of attack of the airfoil. In symbolic form, this pressure differential may be represented as $dp/d\alpha$. A procedure of exactly determining this pressure differential is worked out in great detail in the present analysis. It will be seen that under the aforesaid conditions, it is possible to develop an " exact " method of calculation of the slope of lift curve for a two-dimensional symmetrical airfoil by summing up the local pressure differentials over the airfoil surfaces. It will also be seen that the results of such a calculation differ considerably from the familiar linearized formula $dC_L/d\alpha = 4/\left(M_\infty^2 - 1 \right)^{1/2}$ especially in very high Mach number regions and at Mach number close to 1.00. The Busemann second

and third order theories (Ref. 4) however give a closer agreement with the calculation. Especially, the third order theory which has taken into account the shock wave terms shows a general trend agreeing pretty well with the present calculation. At present, the control surfaces for supersonic missiles and aircraft are generally designed on the basis of the linearized theory. It is hoped that the present calculation may lead to a better design analysis of the control effectiveness. To meet this design need, several charts are presented here which will facilitate the calculation of the slope of lift curve for any two-dimensional symmetrical airfoil in supersonic flow.

Ideal supersonic flow around a two-dimensional symmetrical airfoil :

To clarify the idea of the reader, it is desirable to define here the ideal supersonic flow case that is going to be dealt with in this paper. Fig. 1 represents a section view of a two-dimensional symmetrical airfoil of finite thickness placed parallel to the free stream. The free stream Mach number M_∞ is above 1.00, i. e. supersonic, and the flow is

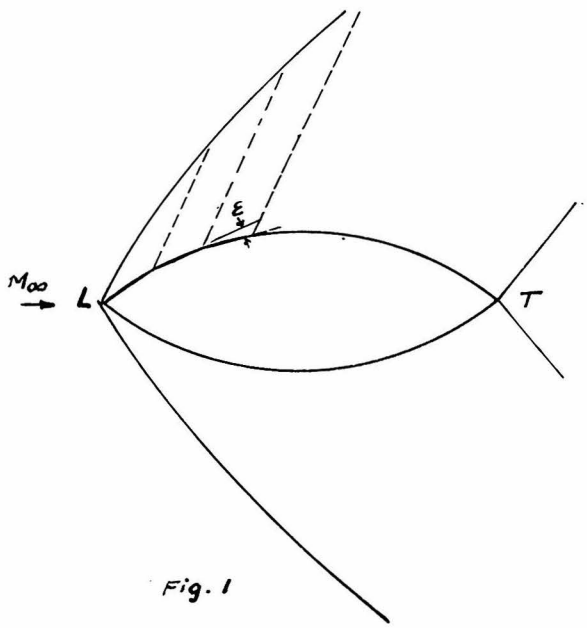

Fig. 1

isentropic before encountering the airfoil. At the leading edge L, locally plane shock waves of equal strength are emitted from both the upper and the lower sides of the airfoil. These shock waves are assumed infinitely thin. They are regarded as an irreversible adiabatic process. The geometry of the airfoil surfaces is assumed known. The airfoil surfaces are continuous arcs which may be considered as composed of a large number of small straight elements intersected at a small angle ε. Neglecting the boundary layer effects, i. e. in potential flow, it can easily be seen that the air in passing from one element to the next element along the airfoil surface will be deflected by an angle ε. The dotted lines in Fig. 1 represent the Mach lines or the characteristic lines emitted from the intersections of the adjacent elements of the airfoil surface. Each Mach line represents a Mach wave which will interfere with the oblique shock wave from L. Through the interference of the Mach waves, the oblique shock waves from L will eventually be transformed into Mach waves extending to infinity. Besides, other Mach waves will be reflected towards the airfoil.. These reflected Mach waves are certainly very weak and in the present analysis their effects are ignored. This is essentially an assumption that the plane oblique shock waves from L will be preserved far enough from the airfoil that the flow may be considered everywhere irrotational behind the shock. In other words, the flow is regarded as isentropic after the shock. Another important limitation is that the complete flow field is assumed supersonic.

With this ideal flow field, it is possible to make an exact analysis of the slope of lift curve of the airfoil by employing the oblique shock laws and the Prandtl-Meyer flow expansion laws.

Fundamental formulae of oblique shock and definition of Prandtl-Meyer angle :

Consider a configuration as in fig. 1 in which a steady uniform supersonic stream with free stream Mach number M_∞ is impinging on a two-dimensional symmetrical airfoil lying parallel to the main stream. Oblique shock waves of equal strength are created at L on both sides of the airfoil. The oblique shock will deflect the flow such that flow direction after the shock is inclined to the main stream at an angle ϕ (Fig. 2). In fig. 2, β denotes the wave angle of the oblique shock, M_2 denotes the local Mach number behind the shock. Knowing M_∞ and ϕ , it is possible to determine β and M_2 by the following oblique shock formulae: (Ref. 1)

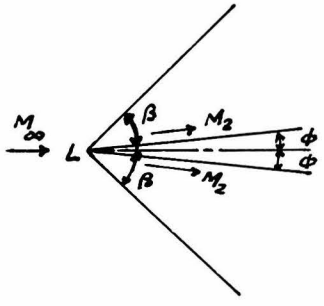

Fig. 2

$$\frac{1}{M_\infty^2} = \sin^2\beta - \frac{\gamma+1}{2}\frac{\sin\beta\sin\phi}{\cos(\beta-\phi)} \qquad (1)$$

$$M_2^2 = \frac{1+\frac{\gamma-1}{2}M_\infty^2}{\gamma M_\infty^2\sin^2\beta - \frac{\gamma-1}{2}} + \frac{M_\infty^2\cos^2\beta}{1+\frac{\gamma-1}{2}M_\infty^2\sin^2\beta} \qquad (2)$$

where γ denotes the ratio of specific heats of air. In the

present calculation γ is taken to be 1.40. M_2 will correspond to a certain Prandtl-Meyer angle θ_2.

The meaning of Prandtl-Meyer angle θ_2 will be clear with an examination of fig. 3. This figure represents a hodograph plane. The region outside the unit Mach number circle (M = 1) represents supersonic flow. If the hodograph of a two-dimensional supersonic flow along a curved wall is plotted on this hodograph plane, it will result in a characteristic curve (an epicycloid). In particular, the curve "ab" in fig. 3 represents the characteristic corresponding to the supersonic expansion flow (sometimes called Prandtl-Meyer flow) with initial flow direction horizontal and initial Mach number one. By "ab", the unique relationship between flow direction and flow velocity, i. e. Mach number is clearly defined. The angle θ indicated in fig. 3 will be called the Prandtl-Meyer angle corresponding to the Mach number M. (Ref. 1) Then, M_2 will correspond to the Prandtl-Meyer angle θ_2 indicated in the figure.

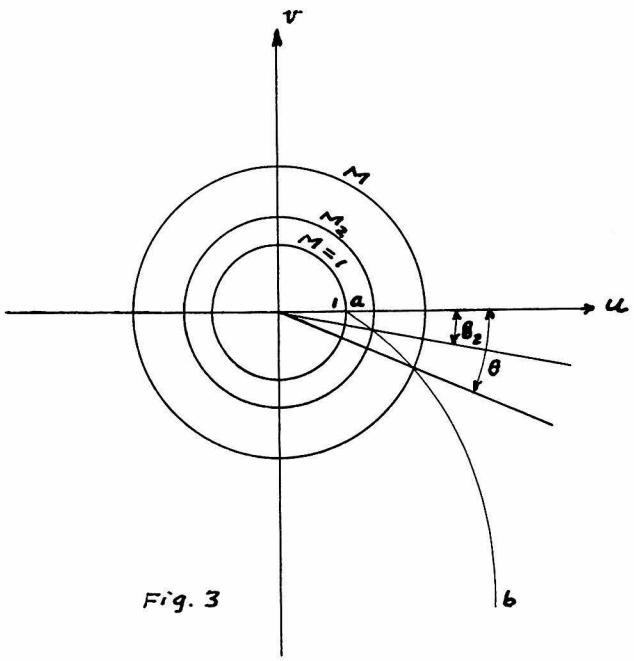

Fig. 3

The supersonic flow around the airfoil is separated by the oblique shock waves into two regions of isentropic flow. Let

$p_{o\infty}$ and p_{o2} represent the stagnation pressures before and after the shock respectively. p_{o2} will be different from $p_{o\infty}$ because of the entropy increase through the introduction of the oblique shock wave. The following formula gives the relation between $p_{o\infty}$ and p_{o2} : (Ref. 1)

$$\frac{p_{o\infty}}{p_{o2}} = \left(\frac{2\gamma}{\gamma+1} M_\infty^2 \sin^2\beta - \frac{\gamma-1}{\gamma+1} \right)^{\frac{1}{\gamma-1}} \left(\frac{(\gamma-1) M_\infty^2 \sin^2\beta + 2}{(\gamma+1) M_\infty^2 \sin^2\beta} \right)^{\frac{\gamma}{\gamma-1}} \qquad (3)$$

The local pressure p_2 on the airfoil surface immediately behind the shock may also be determined by the following formula : (Ref. 1)

$$\frac{p_2}{p_\infty} = \frac{2\gamma}{\gamma+1} M_\infty^2 \sin^2\beta - \frac{\gamma-1}{\gamma+1} \qquad (4)$$

where p_∞ is the free stream pressure.

Therefore the condition at the surface of the airfoil immediately after the oblique shock can be determined. The step-by-step calculation of the airfoil characteristics can be then carried out without great difficulty.

Fundamental formulae for change of local pressure at the airfoil surface due to change in angle of attack :

In fig. 1 the airfoil is placed at an angle of attack of zero degree with respect to the main stream. Let p and M denote the local pressure and Mach number at the airfoil surface. It is known from the characteristics of supersonic flow that local

pressure may be expressed as a function of the local Prandtl-Meyer flow angle θ which is uniquely related to the local Mach number M. In symbolic form, for the flow past the airfoil :

$$\frac{p}{p_{oz}} = f(M) \quad or \quad g(\theta) \tag{5}$$

In potential flow, the local flow direction is everywhere tangential to the airfoil surface. Considering the airfoil surface as made of straight elements (Fig. 4, upper surface), the flow direction at the nth element of the airfoil will differ from the leading edge element of the airfoil by an angle ε_n . ε_n represents the flow expansion angle between the leading edge element and the nth element. Then, the local Prandtl-Meyer angle θ at the nth element of the surface of the airfoil will be given by :

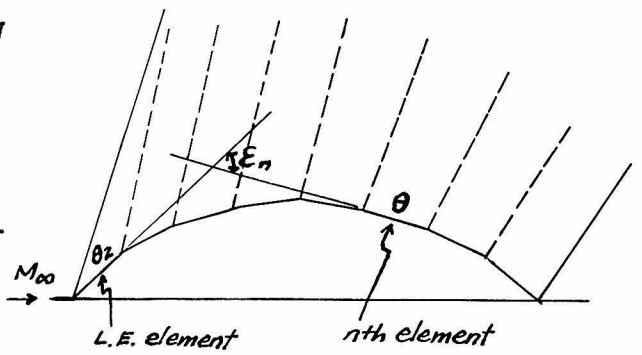

Fig. 4

$$\theta = \theta_z + \varepsilon_n \tag{6}$$

It will be interesting to study the effects of changing the angle of attack of the airfoil, to be more specific, the change of local pressure due to the change of angle of attack. This may be found as follows:

Write :

$$p = p_{oz}\left(\frac{p}{p_{oz}}\right) \tag{7}$$

Differentiating formally with respect to α :

$$\frac{dp}{d\alpha} = p_{o2}\left(\frac{d\ p/p_{o2}}{d\theta}\right)\frac{d\theta}{d\alpha} + \frac{p}{p_{o2}}\frac{dp_{o2}}{d\alpha} \tag{8}$$

But from equation (6):

$$\frac{d\theta}{d\alpha} = \frac{d\theta_2}{d\alpha} \tag{9}$$

Hence,

$$\frac{dp}{d\alpha} = p_{o2}\left(\frac{d\ p/p_{o2}}{d\theta}\right)\frac{d\theta_2}{d\alpha} + \frac{p}{p_{o2}}\frac{dp_{o2}}{d\alpha} \tag{10}$$

Eq. (10) is the fundamental equation of the present report. In eq. (10), the term $(d(p/p_{o2})/d\theta)$ is a function of local Mach number; this can be shown explicitly by introducing the relation for pressure change through a small wave (Ref. 1) :

$$dp = -\rho w^2 \frac{d\theta}{\sqrt{M^2-1}} \tag{11}$$

where ρ , w, M are local density, velocity and Mach number respectively.

This relation can be transformed into the following :

$$d\left(\frac{p}{p_{o2}}\right) = -\frac{\rho w^2}{\gamma p}\frac{\gamma p}{p_{o2}}\frac{d\theta}{\sqrt{M^2-1}}$$

This is readily seen to be expressible as follows :

$$\left(\frac{d\ p/p_{o2}}{d\theta}\right) = -\frac{\gamma p}{p_{o2}}\frac{M^2}{\sqrt{M^2-1}} \tag{12}$$

As can now be easily seen that $dp/d\alpha$ in eq. (10) can be determined for any point on the airfoil provided that the derivatives of θ_2 and p_{o2} with respect to α are known. $d\theta_2/d\alpha$ represents the change in Prandtl-Meyer angle behind the shock at the leading edge element of the airfoil surface due to $d\alpha$.

$dp_{o2}/d\alpha$ represents the change in stagnation pressure behind the oblique shock due to $d\alpha$. In the following sections, these two quantities will be determined.

Determination of $d\theta_2/d\alpha$:

As has been mentioned previously, the θ_2 is determined from M_2 calculated from eqs. (1) and (2). It is possible to write :

$$\frac{d\theta_2}{d\alpha} = \left(\frac{d\theta_2}{dM_2}\right)\left(\frac{dM_2}{d\alpha}\right) = \left(\frac{d\theta_2}{dM_2}\right)\left(\frac{\partial M_2}{\partial \beta}\right)_{M_\infty}\left(\frac{\partial \beta}{\partial \alpha}\right)_{M_\infty} \qquad (13)$$

The determination of derivative of θ_2 with respect to α then can be handled by determination of $d\theta_2/dM_2$, $(\partial M_2/\partial \beta)_{M_\infty}$, $(\partial \beta/\partial \alpha)_{M_\infty}$ separately. However, it is found that dealing with the velocity vector w_2 is more convenient than dealing with the Mach number M_2. Fig. 5 is a flow picture of the oblique shock wave at the leading edge of the airfoil. (upper surface) The components of velocities w_∞ and w_2 before and after the oblique shock respectively are related by the following formulae:

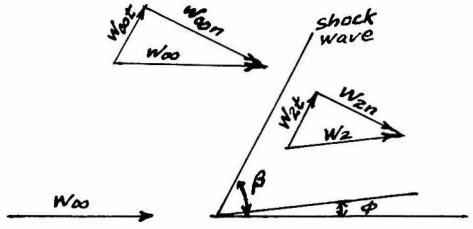

Fig. 5

$$\begin{aligned} w_{\infty n} &= w_\infty \sin\beta \\ w_{\infty t} &= w_\infty \cos\beta \\ &= w_{2t} = w_2 \cos(\beta-\phi) \\ w_{2n} &= w_2 \sin(\beta-\phi) \end{aligned} \qquad (14)$$

The energy equation of the flow upstream of the oblique shock can be written as :

$$\frac{1}{2} w_{\infty n}^2 + \frac{1}{\gamma-1} a_\infty^2 = \frac{\gamma+1}{2(\gamma-1)} a_n^{*2} \qquad (15)$$

where a_∞ is the speed of sound in free stream , i. e. $a_\infty^2 = \gamma p_\infty/\rho_\infty$

and a_n^* is the critical speed of sound in a direction normal to the shock surface. From normal shock theory (Ref. 1), it is known :

$$a_n^{*2} = w_{\infty_n} w_{z_n} \tag{16}$$

Substituting (16) into (15) :

$$w_{\infty_n} w_{z_n} = \frac{2(\gamma-1)}{\gamma+1} \left\{ \frac{1}{2} w_{\infty_n}^2 + \frac{1}{\gamma-1} a_\infty^2 \right\} \tag{17}$$

In (17), a_∞ is held constant, w_{∞_n} and w_{z_n} are however changing with angle of attack of the airfoil. Thus,

$$w_{\infty_n} dw_{z_n} + w_{z_n} dw_{\infty_n} = \frac{2(\gamma-1)}{\gamma+1} \left\{ w_{\infty_n} dw_{\infty_n} \right\}$$

or

$$\frac{dw_{z_n}}{w_{z_n}} + \frac{dw_{\infty_n}}{w_{\infty_n}} = \frac{w_{\infty_n} dw_{\infty_n}}{\frac{1}{2} w_{\infty_n}^2 + \frac{1}{\gamma-1} a_\infty^2}$$

It is thus found :

$$\frac{dw_{z_n}}{w_{z_n}} = \left\{ \frac{w_{\infty_n}^2}{\frac{1}{2} w_{\infty_n}^2 + \frac{1}{\gamma-1} a_\infty^2} - 1 \right\} \frac{dw_{\infty_n}}{w_{\infty_n}} \tag{18}$$

From the relation :

$$w_z^2 = w_{z_n}^2 + w_{z_t}^2$$

it follows that :

$$w_z dw_z = w_{z_n} dw_{z_n} + w_{z_t} dw_{z_t}$$

Introducing the relations in eq. (14), this last equation can be written as :

$$w_z dw_z = w_{z_n} dw_{z_n} + w_{\infty_t} dw_{\infty_t} \tag{19}$$

Also from (14),

$$dw_{\infty n} = w_\infty \cos\beta \, d\beta$$
$$dw_{\infty t} = -w_\infty \sin\beta \, d\beta \qquad (20)$$

From (15) and (16) :

$$w_{2n} = \frac{a_n^{*2}}{w_{\infty n}} = \frac{2(\gamma-1)}{\gamma+1} w_{\infty n}\left[\frac{1}{2} + \frac{1}{\gamma-1}\frac{1}{M_{\infty n}^2}\right] \qquad (21)$$

where $M_{\infty_n} = w_{\infty n}/a_{\infty n}$.

Combining (14), (18), (19), (20) and (21) and reducing, it is finally found :

$$w_2 \, dw_2 = -\frac{4 w_\infty^2 \sin\beta\cos\beta}{(\gamma+1)^2}\left[\gamma + \frac{1}{M_{\infty_n}^4}\right] d\beta \qquad (22)$$

Let $\bar{w} = w/a^*$, i. e. $\bar{w}$ is the velocity ratio to the critical speed of sound. Then,

$$w_2 \left(\frac{dw_2}{d\alpha}\right)_{M_\infty} = a^{*2} \bar{w}_2 \left(\frac{d\bar{w}_2}{d\alpha}\right)_{M_\infty} \qquad (23)$$

From (23) and (22) ,

$$\bar{w}_2 \left(\frac{d\bar{w}_2}{d\alpha}\right)_{M_\infty} = -\frac{4\bar{w}_\infty^2 \sin\beta\cos\beta\left[\gamma + \frac{1}{M_{\infty n}^4}\right]}{(\gamma+1)^2}\left(\frac{\partial\beta}{\partial\alpha}\right)_{M_\infty} \qquad (24)$$

Now in eq. (1), holding M_∞ constant, varying β and ϕ, it is found that :

$$\left\{\sin 2\beta - \frac{\gamma+1}{2}\frac{\sin 2\phi}{2\cos^2(\beta-\phi)}\right\} d\beta - \left\{\frac{\gamma+1}{2}\frac{\sin 2\beta}{2\cos^2(\beta-\phi)}\right\} d\phi = 0$$

or

$$\left(\frac{\partial\phi}{\partial\beta}\right)_{M_\infty} = \frac{4}{\gamma+1}\cos^2(\beta-\phi) - \frac{\sin 2\phi}{\sin 2\beta}$$

It is easily seen that $\phi = \psi - \alpha$ where 2ψ is the vertex angle of the airfoil at the leading edge. (Fig. 6)

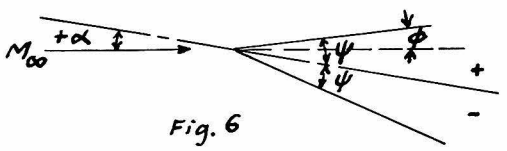

Fig. 6

Then $d\phi/d\alpha = -1$.

Therefore,

$$-\left(\frac{\partial\alpha}{\partial\beta}\right)_{M_\infty} = \frac{4}{\gamma+1}\cos^2(\beta-\phi) - \frac{\sin 2\phi}{\sin 2\beta} \tag{25}$$

Substituting (25) into (24) :

$$\bar{w}_2\left(\frac{d\bar{w}_2}{d\alpha}\right)_{M_\infty} = \frac{4\,\bar{w}_\infty^2 \sin\beta\cos\beta\left[\gamma + \frac{1}{M_{\infty n}^4}\right]}{(\gamma+1)^2\left[\frac{4}{\gamma+1}\cos^2(\beta-\phi) - \frac{\sin 2\phi}{\sin 2\beta}\right]} \tag{26}$$

Introducing the Prandtl-Meyer angle θ_2 now,

$$d\theta_2 = \sqrt{M_2^2 - 1}\,\frac{d\bar{w}_2}{\bar{w}_2}$$

$$\frac{d\theta_2}{d\alpha} = \frac{\sqrt{M_2^2-1}}{\bar{w}_2}\,\frac{d\bar{w}_2}{d\alpha} \tag{27}$$

It follows therefore,

$$\frac{d\theta_2}{d\alpha} = \frac{4\,\frac{\bar{w}_\infty^2}{\bar{w}_2^2}\sin\beta\cos\beta\left[\gamma + \frac{1}{M_{\infty n}^4}\right]\sqrt{M_2^2-1}}{(\gamma+1)^2\left[\frac{4}{\gamma+1}\cos^2(\beta-\phi) - \frac{\sin 2\phi}{\sin 2\beta}\right]} \tag{28}$$

In this equation

$$\frac{\bar{w}_\infty^2}{\bar{w}_2^2} = \frac{\cos^2(\beta-\phi)}{\cos^2\beta}$$

Thus,

$$\frac{d\theta_2}{d\alpha} = \frac{\frac{4}{(\gamma+1)^2}\cos^2(\beta-\phi)\frac{\sin\beta}{\cos\beta}\left[\gamma + \frac{1}{M_{\infty n}^4}\right]\sqrt{M_2^2-1}}{\frac{4}{\gamma+1}\cos^2(\beta-\phi) - \frac{\sin 2\phi}{\sin 2\beta}} \tag{29}$$

In eq. (29), the right-hand side contains four variables ϕ, β, $M_{\infty n}$, and M_2. These four variables are related by the oblique shock wave equations (1) to (4). It is found that for simplicity of computation it would be better to further manipulate eq. (29) such that in its final form only two variables are

involved. In the present presentation, it is felt that the variables $M_{\infty n}$ and M_2 should be expressed in terms of ϕ and β. This can be done as follows :

Write: $M_{\infty n}^2 = M_\infty^2 \sin^2\beta$

From eq. (1) :

$$\frac{1}{M_{\infty n}^2} = 1 - \frac{\gamma+1}{2}\frac{\sin\phi}{\sin\beta\cos(\beta-\phi)} \tag{30}$$

Using this relation, it can be found that :

$$\left(\gamma + \frac{1}{M_{\infty n}^4}\right) = \frac{\gamma+1}{4\sin^2\beta\cos^2(\beta-\phi)}\left[\sin 2\beta \sin 2(\beta-\phi) + (\gamma+1)\sin^2\phi\right] \tag{31}$$

After eliminating M term in (1) and (2), it is found :

$$M_2^2 = \frac{\cos\phi - \dfrac{\sin\phi\sin(\beta-\phi)}{\cos(\beta-\phi)}}{\sin\beta\sin(\beta-\phi) + \dfrac{\gamma-1}{2}\dfrac{\sin\phi\sin(\beta-\phi)}{\cos(\beta-\phi)}}$$

Then,

$$M_2^2 - 1 = \frac{\cos\beta\cos(\beta-\phi) - \dfrac{\gamma+1}{2}\dfrac{\sin\phi\sin(\beta-\phi)}{\cos(\beta-\phi)}}{\sin\beta\sin(\beta-\phi) + \dfrac{\gamma-1}{2}\dfrac{\sin\phi\sin(\beta-\phi)}{\cos(\beta-\phi)}} \tag{32}$$

Putting into eq. (29), finally the following formula is obtained:

$$\frac{d\theta_2}{d\alpha} = \frac{2\left\{\dfrac{\sin 2(\beta-\phi)}{\gamma+1} + \dfrac{\sin^2\phi}{\sin 2\beta}\right\}}{[A]\quad[B]^{\gamma/2}} \tag{33}$$

where

$$[A] = \frac{4}{\gamma+1}\cos^2(\beta-\phi) - \frac{\sin 2\phi}{\sin 2\beta}$$

$$[B] = \left\{\frac{\sin\beta\sin(\beta-\phi) + \dfrac{\gamma-1}{2}\sin\phi\tan(\beta-\phi)}{\cos\beta\cos(\beta-\phi) - \dfrac{\gamma+1}{2}\sin\phi\tan(\beta-\phi)}\right\}$$

It is desired to prepare an engineering chart of $d\theta_2/d\alpha$ vs M_∞. This is done in two steps : first, eq. (33) is used to compute a set of curves of $d\theta_2/d\alpha$ vs β , for each of these curves ϕ is held constant; second, on the set of curves prepared from eq. (33), a set of M_∞ curves computed from eq. (1) is then cross-plotted. From this last cross-plot, a set of $d\theta_2/d\alpha$ vs M_∞ curves for engineering use is prepared. These final curves are presented in this report as fig. 7. The corresponding values of $d\theta_2/d\alpha$ and M_∞ are also tabulated in Table 1.

Determination of $dp_{o2}/d\alpha$:

In previous discussion, it has been pointed out that $d\theta_2/d\alpha$ and $dp_{o2}/d\alpha$ are the two important factors to be determined. The determination of $dp_{o2}/d\alpha$ folows a similar procedure as the determination of $d\theta_2/d\alpha$. It is easily seen from (3) that $p_{o2} = p_{o2}(M_\infty, \beta)$.
Holding M_∞ constant, the derivative of p_{o2} with respect to α may be written as :

$$\frac{dp_{o2}}{d\alpha} = \left(\frac{\partial p_{o2}}{\partial \beta}\right)_{M_\infty} \left(\frac{\partial \beta}{\partial \alpha}\right)_{M_\infty} \tag{34}$$

From (3),

$$p_{o2} = p_{o\infty} \left\{ \frac{2\gamma}{\gamma+1} M_\infty^2 \sin^2\beta - \frac{\gamma-1}{\gamma+1} \right\}^{-\frac{1}{\gamma-1}} \left\{ \frac{\gamma-1}{\gamma+1} + \frac{2}{(\gamma+1) M_\infty^2 \sin^2\beta} \right\}^{-\frac{\gamma}{\gamma-1}} \tag{35}$$

Differentiating (35) with respect to β , it is found that :

$$\left(\frac{\partial p_{o2}}{\partial \beta}\right)_{M_\infty} = p_{o2} \left(\frac{2\gamma}{\gamma^2-1}\right) \frac{\sin 2\beta}{\sin^2\beta} \left[\frac{1}{M_{\infty_n}^2 C} - \frac{M_{\infty n}^2}{D} \right] \tag{36}$$

where $M_\infty^2 \sin^2\beta = M_{\infty n}^2$

$$C = \frac{\gamma-1}{\gamma+1} + \frac{2}{(\gamma+1) M_{\infty n}^2}$$

$$D = \frac{2\gamma}{\gamma+1} M_\infty^2 - \frac{\gamma-1}{\gamma+1}$$

After proper manipulation, it is then found :

$$\left[\frac{1}{M_{\infty n}^2 C} - \frac{M_{\infty n}^2}{D}\right] = -\frac{(\gamma^2-1)}{\left[(\gamma-1)+\frac{2}{M_{\infty n}^2}\right]} \frac{\left(\frac{1}{M_{\infty n}^2}-1\right)^2}{\left[2\gamma - \frac{\gamma-1}{M_{\infty n}^2}\right]} \tag{37}$$

The relation (30) may now be used to express $M_{\infty n}$ in eq. (37) in terms of ϕ and β. After doing this, it is found that (37) is transformed into the following :

$$\left[\frac{1}{M_{\infty n}^2 C} - \frac{M_{\infty n}^2}{D}\right] = -\frac{(\gamma-1)}{4\cos\beta \sin(\beta-\phi)} \frac{\sin^2\phi}{\left[\sin(2\beta-\phi)+\gamma\sin\phi\right]} \tag{38}$$

Combining (25), (34), (36) and (38) :

$$\frac{dp_{oz}}{d\alpha} = \gamma p_{oz} \frac{\sin\phi}{[A][E]} \tag{39}$$

where

$$[A] = \frac{4}{\gamma+1} \cos^2(\beta-\phi) - \frac{\sin 2\phi}{\sin 2\beta}$$

$$[E] = \sin\beta \sin(\beta-\phi)\left[\frac{\sin(2\beta-\phi)}{\sin\phi} + \gamma\right] \tag{40}$$

The preparation of an engineering chart of $dp_{oz}/d\alpha$ vs M_∞ is carried out in two steps just as in the case of $d\theta_z/d\alpha$: first, eq. (39) is used to compute a set of curves of $dp_{oz}/d\alpha$ vs β, for each of these curves ϕ is held constant; second, a set of M_∞ curves computed from eq. (1) is cross-plotted with the set of curves $dp_{oz}/d\alpha$ vs β. From this last cross-plot, a set of $dp_{oz}/d\alpha$ vs M_∞ curves for engineering

use is prepared. These final curves are presented in this report as fig. 8. For computation convenience, $(1/\gamma\, p_{o2})(dp_{o2}/d\alpha)$ rather than $dp_{o2}/d\alpha$ is plotted vs M_∞ in fig. 8; see eq. (46). Corresponding values of $(1/\gamma\, p_{o2})(dp_{o2}/d\alpha)$ and M_∞ are tabulated in Table 1.

"Exact" formula for $dC_L/d\alpha$ at $\alpha = 0°$:

Under the limitations of the ideal flow conditions stated in section 2, it is possible to derive an "exact" formula for $dC_L/d\alpha$ at $\alpha = 0°$ for a two-dimensional symmetrical airfoil. As has been mentioned previously, at $\alpha = 0°$, total pressures on the upper and the lower surfaces of the airfoil are in equilibrium. No lift is exerted on the airfoil at this state. The effect of a purturbation or a momentary change in α is such that this equilibrium is destroyed. It is well-known that in a supersonic flow an airfoil placed at a positive angle of attack α will produce a lift force L. Furthermore, the upper and the lower surfaces of the airfoil contribute equally to this total lift. This fact can be expressed symbolicly as follows:

$$L = -2P \qquad (41)^*$$

*(In (41), P and L are assumed acting parallel; furthermore, in (43), the local p are also considered as acting perpendicular to the free stream. This includes an approximation which will introduce very small error.)

Thus, $$\frac{dL}{d\alpha} = -2\frac{dP}{d\alpha} \qquad (42)$$

where P is the suction existing on the upper surface of the airfoil.

In section 4, it has been shown (fig. 4) that the response of the local pressure p on the upper surface with change in angle of attack $d\alpha$ may be calculated from (10). Combining (10) and (12), it is found:

$$\frac{dp}{d\alpha} = - p_{o_2} \frac{\gamma p}{p_{o_2}} \frac{M^2}{\sqrt{M^2-1}} \frac{d\theta_2}{d\alpha} + \frac{p}{p_{o_2}} \frac{dp_{o_2}}{d\alpha}$$

Integrating along the airfoil chord,

$$\frac{dP}{d\alpha} = - \frac{d\theta_2}{d\alpha} p_{o_2} \int_o^1 \frac{\gamma p}{p_{o_2}} \frac{M^2}{\sqrt{M^2-1}} d\left(\frac{x}{c}\right) + \frac{dp_{o_2}}{d\alpha} \int_o^1 \frac{p}{p_{o_2}} d\left(\frac{x}{c}\right) \qquad (43)$$

where x/c is the ratio of the variable airfoil station to the airfoil chord c, P is the integral of pressure on the upper surface of the airfoil.

Combining (42) and (43) :

$$\frac{dL}{d\alpha} = 2 p_{o_2} \frac{d\theta_2}{d\alpha} \int_o^1 \frac{\gamma p}{p_{o_2}} \frac{M^2}{\sqrt{M^2-1}} d\left(\frac{x}{c}\right) - 2 \frac{dp_{o_2}}{d\alpha} \int_o^1 \frac{p}{p_{o_2}} d\left(\frac{x}{c}\right) \qquad (44)$$

But $L = C_L q_\infty c = \frac{1}{2} C_L \gamma p_\infty M_\infty^2$ (c = unit of length)

$$\frac{dL}{d\alpha} = \frac{1}{2} \gamma p_\infty M_\infty^2 \frac{dC_L}{d\alpha} \qquad (45)$$

Combining (44) and (45), it is thus found :

$$\frac{dC_L}{d\alpha} = \frac{4}{\gamma p_\infty M_\infty^2} \left[p_{o_2} \frac{d\theta_2}{d\alpha} \int_o^1 \frac{\gamma p}{p_{o_2}} \frac{M^2}{\sqrt{M^2-1}} d\left(\frac{x}{c}\right) - \frac{dp_{o_2}}{d\alpha} \int_o^1 \frac{p}{p_{o_2}} d\left(\frac{x}{c}\right) \right]$$

For convenience in computation, this last equation may be written in the form :

$$\frac{dC_L}{d\alpha} = \frac{4}{\frac{p_\infty}{p_{o\infty}} M_\infty^2} \frac{p_{o_2}}{p_{o\infty}} \left[\frac{d\theta_2}{d\alpha} \int_o^1 \frac{p}{p_{o_2}} \frac{M^2}{\sqrt{M^2-1}} d\left(\frac{x}{c}\right) - \frac{1}{\gamma p_{o_2}} \frac{dp_{o_2}}{d\alpha} \int_o^1 \frac{p}{p_{o_2}} d\left(\frac{x}{c}\right) \right] \qquad (46)$$

This is the "exact" formula compatible with the ideal conditions defined in section 2. The computation of $dC_L/d\alpha$ at $\alpha = 0^\circ$ now

resolves into the evaluation of two integrals:

$$\frac{d\theta_2}{d\alpha}\int_0^{'}\frac{p}{p_{o2}}\frac{M^2}{\sqrt{M^2-1}}\,d\left(\frac{x}{c}\right) \quad \text{and} \quad \frac{1}{\gamma p_{o2}}\frac{dp_{o2}}{d\alpha}\int_0^{'}\frac{p}{p_{o2}}\,d\left(\frac{x}{c}\right) \quad .$$

Using figs. 7 and 8 with a set of Prandtl-Meyer flow charts (as the standard set prepared by GALCIT), this can be done without great difficulty. Indeed, after being used to the procedure, the evaluation of the integrals can be quickly done by an engineer with the labour of an hour or two. Since this is an "exact" solution of the flow state defined in section 2, it is expected the result of calculation from (46) will be more accurate than the linearized or the second order or the third order theories. This will be discussed in the following sections.

Discussion on $d\theta_2/d\alpha$ and $dp_{o2}/d\alpha$:

Before going into illustrative examples showing the applications of eq. (46), it is felt that a few more words on the behavior of the $d\theta_2/d\alpha$ and $dp_{o2}/d\alpha$ curves will be helpful.

As has been mentioned in section 2, the present method is restricted to completely supersonic flow only. Thus the limiting case will be when the Mach number immediately behind the shock, M_2, becomes 1.00. For if the Mach number behind the shock, M_2, is less than 1.00, there will be a subsonic flow region in the flow, and the differential equation governing the subsonic flow is of the elliptic type. The characteristics of this flow are not real. The disturbance at one point will be propagated forward into the fluid. The present analysis

will therefore break down.

It will be clearer to state the limiting cases in the following manner:

1. For a certain given airfoil with given vertex angle ψ, there exists a minimum free stream Mach number $M_{\infty m}$, such that with free stream Mach number M_∞ lower than $M_{\infty m}$, the present method will not apply.

2. Alternatively, if the free stream Mach number M_∞ is fixed, there will an airfoil with a vertex angle ψ_m, such that for any airfoil with vertex angle ψ greater than ψ_m, the present method does not apply.

Now, it will be interesting to study the behavior of $d\theta_2/d\alpha$ and $dp_{o2}/d\alpha$ in this limiting case, namely, when $M_2 = 1.00$.

From (27),

$$\frac{d\theta_2}{d\alpha} = -\frac{\sqrt{M_2^2-1}}{\bar{w}_2}\frac{d\bar{w}_2}{d\phi}$$

when $M_2 = 1.00$, $\frac{\sqrt{M_2^2-1}}{\bar{w}_2} = 0$

But $d\bar{w}_2/d\phi$ remains finite. This fact can be seen easily from the oblique shock polar (fig. 9). This oblique shock polar is actually a hodograph diagram of the oblique shock flow field. $\bar{w}_2$ represents a velocity vector with horizontal and vertical components of $\bar{u}_2$ and $\bar{v}_2$ respectively. It is clear that when point A is moving along the shaded (supersonic) portion of the polar, $\bar{w}_2$ will be

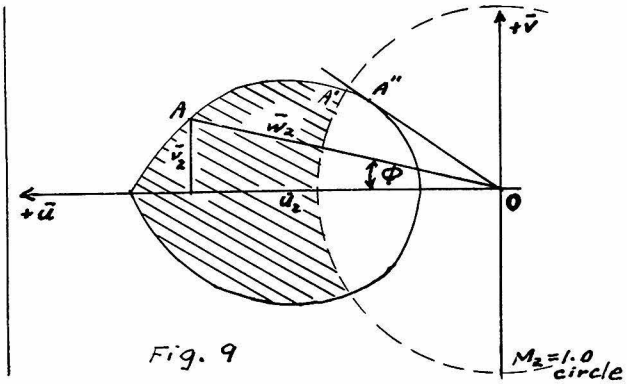

Fig. 9

monotonicly decreasing as ϕ increases. $d\bar{w}_2/d\phi$ at A' ($M_2 = 1.00$) will be negative but finite. A" is the point representing maximum possible deflection of the flow without occurence of detached shock wave. It is concluded therefore, $d\theta_2/d\alpha = 0$ when $M_2 = 1.00$.

The values of $dp_{o2}/d\alpha$ have been actually computed for the case of $M_2 = 1.00$; the values are given in Table 1. They are all positive finite values.

Referring back to (46), it is easily seen that in the limiting case $M_2 = 1.00$ the first integral vanishes leaving a negative quantity arising from the second integral. Hence, $dC_L/d\alpha$ at $\alpha = 0^\circ$ for this limiting case becomes negative; this reslt will be discussed later.

<u>$dC_L/d\alpha$ formulae from approximate theories</u> :

In the following section, illustrative examples are computed from the present "exact" formula (46). For the purpose of comparison, the Ackeret's linearized theory (Ref. 1) and the Busemann's second order and third order approximation theories (Ref. 4) are studied. It is found that Busemann's calculation of the coefficients of the approximate series for the pressure change due to flow deflection in isentropic flow and in oblique shock flow involved several errors. The error in the case of the approximation series for oblique shock flow was discovered lately by E. V. Laitone (Ref. 3). Laitone's new derivation has been checked. Busemann's mistake in the

isentropic flow case has been corrected. (For details see Appendix.) With these corrections, the approximate formulae for $dC_L/d\alpha$ of the two-dimensional symmetrical airfoil will take the following forms:

Linearized theory :

$$\frac{dC_L}{d\alpha} = 2c_1 \tag{47}$$

Second order theory :

$$\frac{dC_L}{d\alpha} = \left(2+\frac{4}{3}\tau^2\right)c_1 \tag{48}$$

Third order theory :

$$\frac{dC_L}{d\alpha} = \left(2+\frac{4}{3}\tau^2\right)c_1 + \left(c_3-\frac{c_1}{2}\right)8\tau^2 - 24d\tau^2 \tag{49}$$

where τ = maximum thickness/chord

i. e. thickness ratio (50)

$$c_1 = \frac{2}{\sqrt{M_\infty^2-1}} = b_1 \tag{51}$$

$$c_2 = \frac{1}{(M_\infty^2-1)^2}\left\{\frac{\gamma+1}{2}M_\infty^4 - 2M_\infty^2 + 2\right\} = b_2 \tag{52}$$

$$c_3 = \frac{1}{(M_\infty^2-1)^{7/2}}\left\{\left(\frac{1+\gamma}{6}\right)M_\infty^8 + \left(\frac{2\gamma^2-7\gamma-5}{6}\right)M_\infty^6 + \frac{5}{3}(1+\gamma)M_\infty^4 - 2M_\infty^2 + \frac{4}{3}\right\} \tag{53}$$

$$b_3 = \frac{1}{(M_\infty^2-1)^{7/2}}\left\{\frac{(1+\gamma)^2}{16}M_\infty^8 - \left(\frac{-3\gamma^2+12\gamma+7}{12}\right)M_\infty^6 + \frac{3}{2}(1+\gamma)M_\infty^4 - 2M_\infty^2 + \frac{4}{3}\right\} \tag{54}$$

$$d = c_3 - b_3 \tag{55}$$

In (51) to (55), the c_1 , c_2 , c_3 and b_1 , b_2 , b_3 are respectively the coefficients of the first three terms in the following infinite series expressions for the pressure coe-

fficients C_{P_i} and C_{P_s} corresponding to the flow deflection angle ϕ in the isentropic flow case and in the oblique shock flow case respectively, namely,

Definition of pressure coefficient:

$$C_p = \frac{p - p_\infty}{\frac{1}{2}\rho_\infty w_\infty^2} \tag{56}$$

Isentropic flow :

$$C_{P_i} = \sum_{n=1}^{\infty} c_n \phi^n = c_1 \phi + c_2 \phi^2 + c_3 \phi^3 + \cdots \tag{57}$$

Oblique shock flow :

$$C_{P_s} = \sum_{n=1}^{\infty} b_n \phi^n = b_1 \phi + b_2 \phi^2 + b_3 \phi^3 + \cdots \tag{58}$$

The values of c_1 , c_2 , c_3 are computed for various M_∞ and tabulated in Table 2, in which also values of b_3 taken from Laitone's paper are included. d represents the difference between the coefficients of third terms in the approximation series (57) and (58). Thus, d actually represents the effect of the oblique shock wave. And, therefore, it is evident from (47), (48) and (49) that:

1. In linearized theory the airfoil is assumed of zero thickness and the flow around the airfoil is everywhere supersonic and isentropic.

2. In second order theory the airfoil is assumed of finite thickness and the flow around the airfoil is everywhere supersonic and isentropic. The effects of thickness is expressed in the term involving τ^2.

3. In third order theory the airfoil is assumed of finite thickness and the airfoil introduces oblique shock waves in the flow which is however isentropic before and after the

oblique shock and everywhere supersonic. The effects of thickness and shock waves are expressed in the terms involving τ^2 and d.

In the present theory, the flow around a two-dimensional symmetrical airfoil of finite thickness is considered with the presence of oblique shock waves. Hence, it is expected that the third order theory will show a better agreement with the present thoery. This will be seen to be true in the following calculations for two simple cases.

Illustrative examples :

The present theory is used to compute the $dC_L/d\alpha$ at $\alpha = 0^\circ$ for two cases, namely, 1. a symmetrical circular arc airfoil of 5% thickness, and 2. a symmetrical circular arc aiffoil of 10% thickness. In both cases, the computation procedure may be outlined as follows :

1. Determination of geometry of the airfoil surface :

In the present method of calculation, it is evident that the accuracy of the results depends on the care given in the determination of the geometry of the airfoil surface. For the illustrative examples included in this report, the circular arc surfaces are approximated by 20 straight line elements. For greater accuracy, a higher number of elements may be used. In general, for a circular arc airfoil, the following formulae hold : The half vertex angle of the airfoil, ψ , (fig. 10)

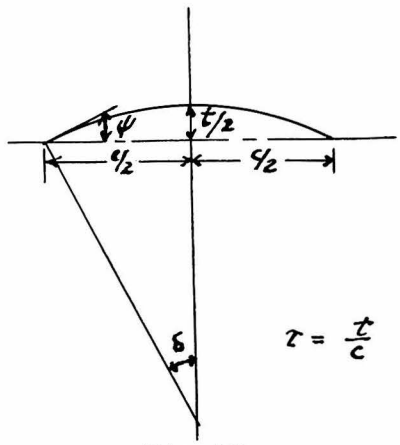

Fig. 10

$$\psi = \delta\left(1 - \frac{1}{N}\right) \tag{59}$$

where $\delta = \sin^{-1}\frac{2\tau}{1+\tau^2}$

τ is the thickness ratio of the given airfoil, N is the number of straight elements to be used in the approximation. For $\alpha = 0^\circ$, $\psi = \phi$.

The expansion angle between successive straight elements is determined by the formula :

$$\varepsilon = \frac{2\delta}{N} \tag{60}$$

For any other given airfoil shape, the vertex angle ψ and the expansion angle ε can be found also. In such cases, proper formulae should be determined in substitution of (59) and (60).

2. Determination of the conditions immediately after shock:

The flow deflection angle ϕ at the leading edge element being determined by (59), it is now possible to use (1) and (2) to determine β and M_2 for given M_∞. Another method is to determine β from an oblique shock chart. (Ref. 1) Then compute p_2/p_∞ from (4). Compute $p_{o\infty}/p_{o2}$ from (3). And compute $p_\infty/p_{o\infty}$ by the familiar formula :

$$\frac{p}{p_o} = \left[1 + \frac{\gamma-1}{2}M^2\right]^{-\frac{\gamma}{\gamma-1}} \tag{61}$$

Combining these results to find p_2/p_{o2} , namely,

$$\frac{p_2}{p_{o2}} = \frac{p_2}{p_\infty}\,\frac{p_\infty}{p_{o\infty}}\,\frac{p_{o\infty}}{p_{o2}}$$

Again using (61), it is possible to determine M_2 . This second procedure is used in actually carrying out the present

examples because $p_{o\infty}/p_{oz}$ and $p_\infty/p_{o\infty}$ charts are available in GALCIT and therefore the computations involved in the second method seem to be easier than applying (1) and (2) directly. (M_z may also be read directly from oblique shock charts but the accuracy will be poorer.) After M_z is determined, the corresponding Prandtl-Meyer angle θ_z is read from the Prandtl-Meyer flow charts. These computations have been carried out for a series of M_∞'s for both the 5% thick airfoil and the 10% thick airfoil.

3. Determination of the integral $\int_0^1 \frac{p}{p_{oz}}\, d(\frac{x}{c})$:

The next step is to find local Prandtl-Meyer angle θ at successive elements of the airfoil surface. This can be easily done using (6). The standard p/p_{oz} vs θ charts (as prepared in GALCIT) are now used to find p/p_{oz} existing over the various elements. These readings of p/p_{oz} can be plotted against x/c and the area under the curve (fig. 11) can be graphically integrated. In the present calculation, the p/p_{oz} values existing over the twenty elements are averaged over the entire surface, and the area under the rectangle with height of $(p/p_{oz})_{av.}$ is taken to be equal to the integral. This calculation has been repeated at a number of M_∞'s for both the 5%thick airfoil and the 10% thick airfoil.

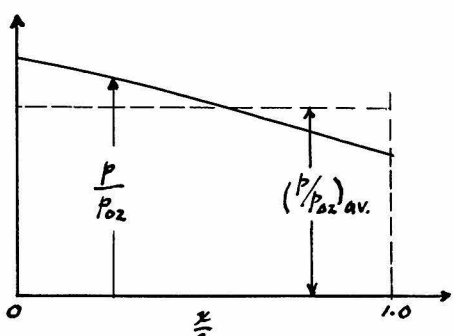

Fig. 11

4. Determination of the integral $\int_0^1 \frac{p}{p_{oz}} \frac{M^2}{\sqrt{M^2-1}}\, d(\frac{x}{c})$:

Knowing the local Prandtl-Meyer angle θ at the successive elements of the airfoil surface, the local Mach number M can be found from standard M vs θ charts. Calculate the factor $M^2 / (M^2 - 1)^{1/2}$ and multiply it by p/p_{o2} found in step 3. And then the quantity $\frac{p}{p_{o2}} \frac{M^2}{\sqrt{M^2-1}}$ can be plotted against x/c resulting in a diagram like fig. 12. Then the integral is evaluated at a number of M_∞'s by the same approximation procedure as in step 3.

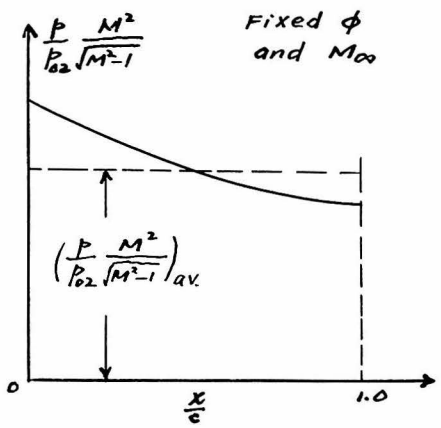

Fig. 12

5. Determination of $d\theta_2/d\alpha$ and $1/\gamma \frac{p}{o2}(dp_{o2}/d\alpha)$:

For the known flow deflection ϕ and at the various free stream Mach numbers used in the foregoing steps, the values of $d\theta_2/d\alpha$ and $(1/\gamma \frac{p}{o2})(dp_{o2}/d\alpha)$ are read from figs. 8 and 7.

6. Determination of $dC_L/d\alpha$:

Finally the values found in the previous steps are substituted in (46) and the values of $dC_L/d\alpha$ are calculated.

These computation results are given in Tables 3 and 4. It should be pointed out at last that the computations though a little tedious are very straight forward and with the help of standard oblique shock charts and Prandtl-Meyer flow charts very rarely any errors in the intermediate steps will be likely to occur. For completeness, the basic formulae for computation of the Prandtl-Meyer flow charts are given below. (Ref. 1)

$$\frac{p}{p_o} = \left(1 + \frac{\gamma-1}{2} M^2\right)^{-\frac{\gamma}{\gamma-1}} \qquad (61)$$

$$\theta = \sqrt{\frac{\gamma+1}{\gamma-1}}\tan^{-1}\sqrt{\frac{\gamma-1}{\gamma+1}}\sqrt{M^2-1} - \tan^{-1}\sqrt{M^2-1} \qquad (62)$$

It will be found in Tables 3 and 4 that $dC_L/d\alpha$ values computed from the approximate formulae (47),(48), and (49) are also listed for comparison. The computation procedures for these approximation theories are self-evident and no further elaborations are needed. The data from Tables 3 and 4 are plotted in figs. 13 and 14. It is possible to draw the following conclusions from the results of computations.

Conclusion :

1. The famous linearized theory formula gives a value of $dC_L/d\alpha$ too low in comparison with the present theory. The difference becomes very great at very high Mach number region. In extreme case like the 10% thick airfoil at free stream Mach number of 8.00, the $dC_L/d\alpha$ obtained from linearized theory is about 50% lower than the $dC_L/d\alpha$ from the present theory. Furthermore, by comparing the second order theory with the present ~~the present~~ theory, it is seen that the second order theory has very little improvement over the linearized theory. It may therefore be concluded that this enormous difference in $dC_L/d\alpha$ between the "exact" theory and the linearized theory is mostly due to the shock effects. This conclusion is substantiated by the fact that the Busemann's third order theory which includes a shock wave term, brings the $dC_L/d\alpha$ values at various Mach numbers in much better agreement with the present theory. (Even in the

extreme case of very high Mach number , say $M_\infty = 8.00$, for the 10% thick airfoil, the discrepancy is about 25%.)

2. The thickness of airfoil, however, to some extent, determines the strength of the shock wave. For thinner airfoil, the oblique shock wave produced will be weaker. Thus, if comparison is made between two airfoils of different thicknesses at same free stream Mach number, it will be expected that for the thinner airfoil, the difference between the "exact" theory and the approximate theories will be smaller. This is proved to be true by the present calculations.

3. From the present theory, the slope of lift curve will reverse its sign in the lower Mach number region. This is due to the vanishing of $d\theta_2/d\alpha$ at the limiting case, $M_2 = 1.00$. A study of the behavior of the integrals $\frac{1}{\gamma p_{02}} \frac{dp_{02}}{d\alpha} \int_0^1 \frac{p}{p_{02}} d\left(\frac{x}{c}\right)$ and $\frac{d\theta_2}{d\alpha} \int_0^1 \frac{p}{p_{02}} \frac{M^2}{\sqrt{M^2-1}} d\left(\frac{x}{c}\right)$ shows that as the free stream Mach number decreases both integrals increases in magnitude and always the second integral dominates except when the region close to the limiting case is reached. In the region near the limiting case, the second integral decreases violently due to the variation of $d\theta_2/d\alpha$ while the first integral is comparatively very stable. Thus, the values of $dC_L/d\alpha$ are dominated by the second integral at all Mach numbers except those Mach numbers close to the limiting case. The first integral expresses the effect of change in stagnation pressure behind the oblique shock. This integral accounts for the effect of change of entropy. In other words, it may be asserted that the reversal of sign in the slope of lift curve at Mach number close to 1.00 is a result

from the oblique shock effects. In linearized theory and second order theory, the oblique shock waves are ignored, thus, this tendency of reversal in sign in $dC_L/d\alpha$ is obscured. This fact is further substantiated by a calculation of the slope of lift curve near Mach number of 1.00 using the third order theory. The third order theory actually shows the same tendency only the occurence of the reversal of sign is at a Mach number still closer to $M_\infty = 1.00$. This is explainable by the fact that the third order theory has not been able to account for the oblique shock effects completely due to the omission of higher order terms. The reversal of sign in $dC_L/d\alpha$ is actually observed in certain recent experimental study of the airfoil characteristics in transonic regions. It is hereby shown that this behavior of the airfoil is explainable by a potential theory with proper assumptions regarding the oblique shock.

4. In the present calculation, it has been stressed that the lower limit is the case in which $M_2 = 1.00$. There appears to be no limit in the high Mach number end. However, it must be remembered that the irrotationality of the flow behind the shock is a very essential postulate. If this postulate is violated the theory will break down. Thus, as a general rule, it may be stated that for thinner airfoil the theory will find its application extended further in the direction of the high Mach number end. For thick airfoil, the results of calculation from the present theory may not be so accurate at very high Mach numbers because the flow behind the shock in such cases may be rotational. However, for such cases, the linear theory certainly

does not apply.

5. Lastly, it should be pointed out that effects of viscosity are completely ignored in the present analysis. The effects of viscosity may be important in determining the local flow conditions. And from recent reseaches, it has been found out that in transonic regions the nature of the shock wave depends to a large extent on the nature of the boundary layer.

List of references :

1. H. W. Liepmann and A. E. Puckett : Introduction to Aerodynamics of a Compressible Fluid, Wiley, 1947

2. G. I. Taylor and J. W. Maccoll : The Mechanics of Compressible Fluids, Aerodynamic Theory vol. 3, 1934

3. E. V. Laitone : Exact and Approximate Solutions of Oblique Shock Waves, Journal of Aero. Sciences, Jan. 1947

4. A. Busemann : Volta Congress, pp. 328-360, 1936

Table 1

$\Phi = 20^\circ$			$\Phi = 8^\circ$		
M_∞	$d\theta_2/d\alpha$	$\frac{1}{\gamma p_{02}} \frac{dp_{02}}{d\alpha}$	M_∞	$d\theta_2/d\alpha$	$\frac{1}{\gamma p_{02}} \frac{dp_{02}}{d\alpha}$
1.825	0	.730	1.36	0	.151
2	1.409	.360	2	1.063	.061
3	1.485	.571	3	1.101	.150
4	1.633	.968	4	1.154	.307
5	1.787	1.418	5	1.218	.526
6	1.92	1.840	6	1.287	.800
7	2.039	2.242	7	1.360	1.152
8	2.14	2.607	8	1.436	1.570
9	2.228	2.900	9	1.510	2.000
10	-----	3.168	10	1.580	2.450
$\Phi = 16^\circ$			$\Phi = 4^\circ$		
1.672	0	.463	1.21	0	.0595
2	1.246	.210	2	1.017	.020
3	1.331	.428	3	1.028	.040
4	1.458	.765	4	1.043	.090
5	1.60	1.185	5	1.063	.170
6	1.735	1.660	6	1.084	.270
7	1.856	2.120	7	1.111	.410
8	1.962	2.560	8	1.141	.580
9	2.053	2.960	9	1.171	.780
10	2.127	3.320	10	1.203	1.020
$\Phi = 12^\circ$					
1.51	0	.281			
2	1.137	.122			
3	1.204	.280			
4	1.299	.550			
5	1.409	.905			
6	1.518	1.330			
7	1.628	1.790			
8	1.733	2.258			
9	1.826	2.740			
10	1.902	3.180			

Table 2

M_∞	1.1	1.2	1.3	1.4	1.5	1.6
c_3	867	53.8	14.40	5.80	3.06	1.97
d	322.6	.58	.13	.328	.271	.183
c_1	4.364	3.015	2.41	2.05	1.79	1.60
c_2	30.32	8.31	4.30	2.92	2.29	1.95

M_∞	2.0	3.0	4.0	5.0	10.0
c_3	.927	1.13	1.51	1.91	3.9
d	.092	.061	.105	.136	.322
c_1	1.16	.707	.516	.408	.201
c_2	1.47	1.27	1.23	1.22	1.204

Table 3

5% thick symmetrical circular arc airfoil

M_∞	$dC_L/d\alpha$ "exact" (46)	$dC_L/d\alpha$ Linearized (47)	$dC_L/d\alpha$ 2nd. order (48)	$dC_L/d\alpha$ 3rd. order (49)
1.1	----	8.728	8.728	6.628
1.2	----	6.030	6.036	7.047
1.278	- .198	5.000	5.000	5.050
1.4	4.190	4.096	4.100	4.178
2.0	2.36	2.310	2.312	2.314
4.0	1.13	1.033	1.034	1.053
6.0	.757	.676	.677	.707
8.0	.649	.504	.505	.548

Table 4

10% thick symmetrical circular arc airfoil

M_∞	$dC_L/d\alpha$ "exact" (46)	$dC_L/d\alpha$ Linearized (47)	$dC_L/d\alpha$ 2nd. order (48)	$dC_L/d\alpha$ 3rd. order (49)
1.1	----	-----	----	.461
1.4	----	4.096	4.111	4.572
1.465	- .435	-----	----	----
2.0	2.545	2.310	2.319	2.369
4.0	1.261	1.033	1.037	1.112
6.0	.995	.676	.679	.800
8.0	.907	.504	.506	.678

Fig. 7 $\frac{d\theta_2}{d\alpha}$ vs M_∞

Derivative of Prandtl-Meyer Angle θ_2 Behind Oblique Shock

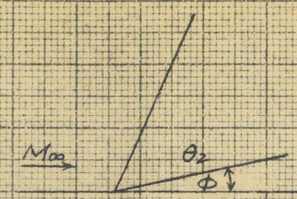

Fig 8 DERIVATIVE OF STAGNATION PRESSURE BEHIND OBLIQUE SHOCK

$+\frac{1}{\gamma P_{02}}\frac{dP_{02}}{d\alpha}$ vs M_∞

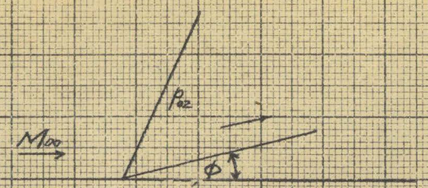

$\phi=20°$ $\phi=16°$ $\phi=12°$ $\phi=8°$ $\phi=4°$

$\frac{1}{\gamma P_{02}}\frac{dP_{02}}{d\alpha}$

2.5 2.0 1.5 1.0 0.5 0

1 2 3 4 5 6 7 8 9 10

M_∞

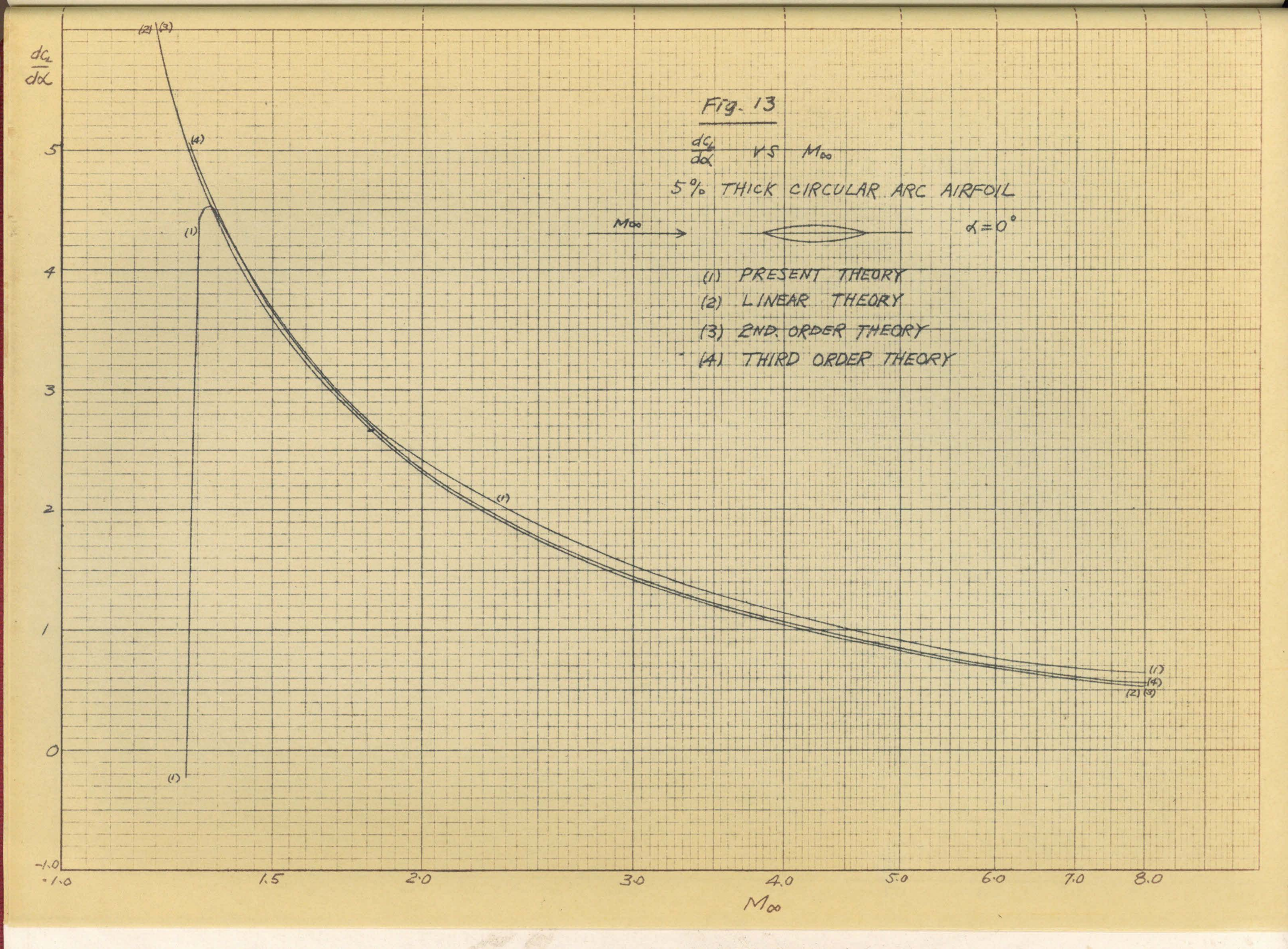
Fig. 13
$\frac{dC_L}{d\alpha}$ VS M_∞
5% THICK CIRCULAR ARC AIRFOIL
M_∞
$\alpha = 0°$
(1) PRESENT THEORY
(2) LINEAR THEORY
(3) 2ND. ORDER THEORY
(4) THIRD ORDER THEORY
$\frac{dC_L}{d\alpha}$
M_∞
-1.0
1
2
3
4
5
1.5
2.0
3.0
4.0
5.0
6.0
7.0
8.0

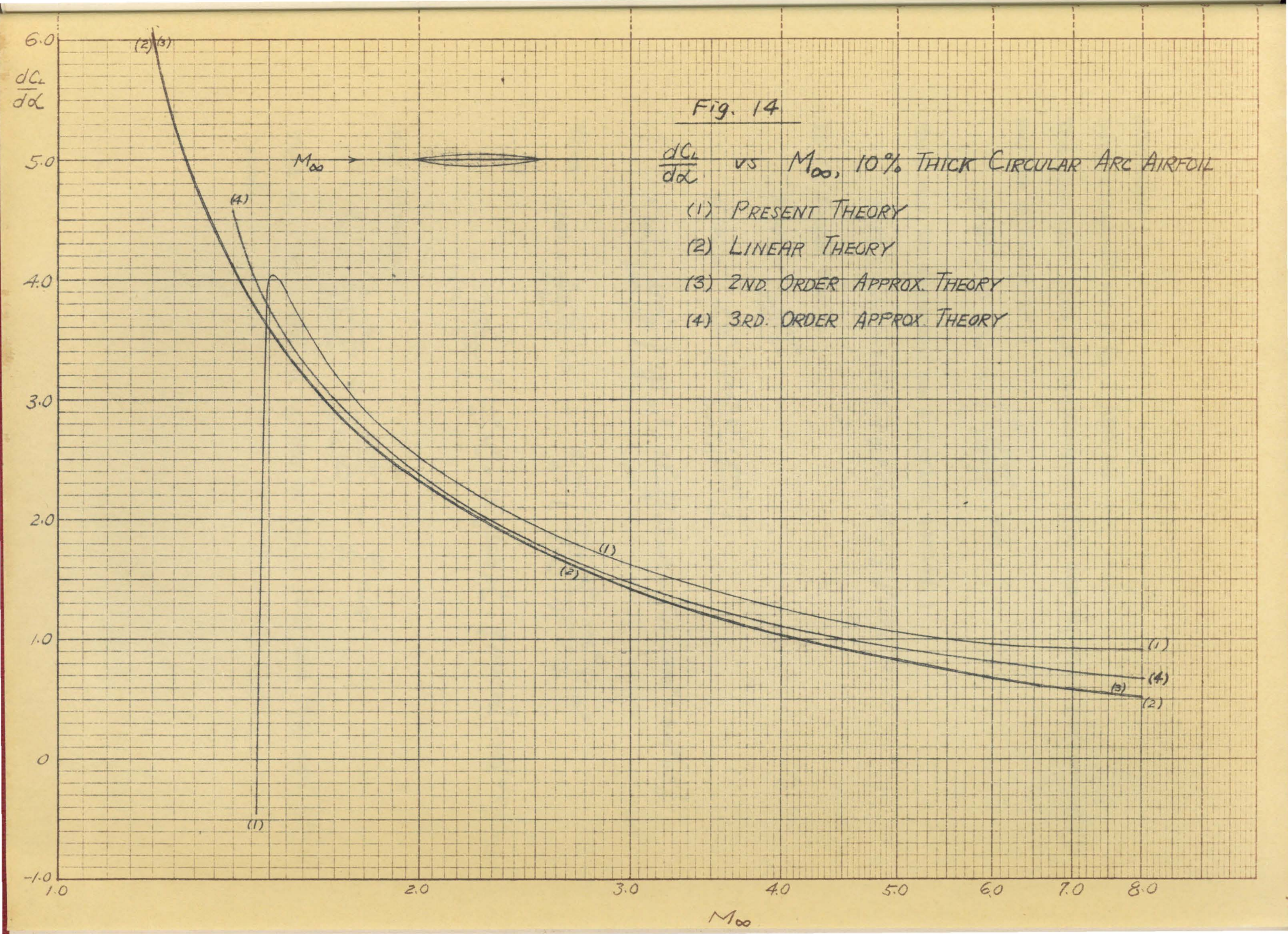
Fig. 14
$\frac{dC_L}{d\alpha}$ vs M_∞, 10% Thick Circular Arc Airfoil
(1) Present Theory
(2) Linear Theory
(3) 2nd. Order Approx. Theory
(4) 3rd. Order Approx. Theory
$\frac{dC_L}{d\alpha}$
M_∞
6.0
5.0
4.0
3.0
2.0
1.0
0
-1.0
1.0
2.0
3.0
4.0
5.0
6.0
7.0
8.0

Appendix :

Derivation of c_1 , c_2 , and c_3 :

The pressure rise in isentropic flow due to flow deflection ϕ may be written as :

$$p(\phi) = p - p_\infty = \int_0^\phi \frac{\rho w^2}{\sqrt{M^2-1}}\, d\phi$$

This may be expanded as a Taylor series :

$$p(\phi) = p(0) + p'(0)\phi + \frac{1}{2}p''(0)\phi^2 + \frac{1}{6}p'''(0)\phi^3 + \cdots$$

It is found that :

$$p'(\phi) = \frac{\rho w^2}{\sqrt{M^2-1}}$$

$$p''(\phi) = \frac{\rho w^2}{2}\left[\frac{(M^2-2)^2+\gamma M^4}{(M^2-1)^2}\right]$$

$$p'''(\phi) = \frac{2\rho w^2}{(M^2-1)^{7/2}}\left\{\frac{1+\gamma}{4}M^8 + \frac{2\gamma^2-7\gamma-5}{4}M^6 + \frac{5}{2}(1+\gamma)M^4 - 3M^2 + 2\right\}$$

Thus

$$p(\phi) = \frac{\rho_\infty w_\infty^2}{\sqrt{M_\infty^2-1}}\phi + \frac{\rho_\infty w_\infty^2}{4}\left[\frac{(M_\infty^2-2)^2+\gamma M_\infty^4}{(M_\infty^2-1)^2}\right]\phi^2$$

$$+ \frac{2\rho_\infty w_\infty^2}{6(M_\infty^2-1)^{7/2}}\left\{\frac{1+\gamma}{4}M_\infty^8 + \frac{2\gamma^2-7\gamma-5}{4}M_\infty^6 + \frac{5}{2}(1+\gamma)M_\infty^4 - 3M_\infty^2 + 2\right\}$$

Now introduce :

$$C_{pi} = \frac{p-p_\infty}{\frac{1}{2}\rho_\infty w_\infty^2} = \frac{p(\phi)}{\frac{1}{2}\rho_\infty w_\infty^2} = \sum_{n=1}^{\infty} c_n \phi^n$$

Then c_1 , c_2 , and c_3 given in (51), (52) and (53) are easily found.